

Noise dephasing in the edge states of the Integer Quantum Hall regime

P. Roulleau, F. Portier, and P. Roche

*CEA Saclay, Service de Physique de l'Etat Condensé,
Nanoelectronic group, F-91191 Gif-sur-Yvette, France*

A. Cavanna, G. Faini, U. Gennser, and D. Mailly

*CNRS, Laboratoire de Photonique et Nanostructures,
Phynano team, Route de Nozay, F-91460 Marcoussis, France*

(Dated: April 19, 2022)

An electronic Mach Zehnder interferometer is used in the integer quantum hall regime at filling factor 2, to study the dephasing of the interferences. This is found to be induced by the electrical noise existing in the edge states capacitively coupled to each others. Electrical shot noise created in one channel leads to phase randomization in the other, which destroys the interference pattern. These findings are extended to the dephasing induced by thermal noise instead of shot noise: it explains the underlying mechanism responsible for the finite temperature coherence time $\tau_\varphi(T)$ of the edge states at filling factor 2, measured in a recent experiment. Finally, we present here a theory of the dephasing based on Gaussian noise, which is found in excellent agreement with our experimental results.

Although many experiments in quantum optics can be reproduced with electron beams using the edge states of the Integer Quantum Hall Effect (IQHE), there exist fundamental differences due to the Coulomb interaction. As an example, the Mach-Zehnder type of interferometer in the IQHE [1] has recently allowed to observe quantum interferences with the unprecedented 90% visibility [2], opening a new field of promising quantum information experiments. Indeed, the edge states of the IQHE provide a way to obtain 'ideal' uni-dimensional quantum wires. However, very little is known about the decoherence processes in these 'ideal' wires. Only very recently their coherence length was quantitatively determined as well as its temperature dependence established [3]. Here, we show that the underlying mechanism responsible for the finite coherence length is the thermal noise combined with the poor screening in the IQHE regime [4].

In the IQHE, gapless excitations develop on the edge of the sample and form one dimensional chiral wires (edge states), the number of which is determined by the number of electrons per quantum of flux (the filling factor ν). In these wires, the electrons drift along the edge in a beam-like motion making experiments usually done with photons possible with electrons. The choice of the filling factor at which one obtains high visibility interferences requires a compromise between a magnetic field high enough to form well defined edge states, and small enough to still deal with a good Fermi liquid. Naïvely one could think that the highest visibility would have been observed at $\nu = 1$, but it is not actually the case [1]. This is most probably due to decoherence induced by low energy collective spin excitations (skyrmions [5]) making spin flip processes possible. In practice, the highest visibility (90% [2]) has been obtained at filling factor 2, when there are two spin polarized edge states. Here, chirality and uni-dimensionality prevent first order inelastic scat-

tering in the wires themselves [6], while tunneling from one edge to the other requires spin flip [7].

To show that the origin of the finite coherence length is related to the coupling between two neighbouring edge states, we have proceeded as follow. First we have made a which-path experiment inducing on purpose shot noise on the inner channel while measuring the outer channel interferences. The visibility decrease is shown to result from a gaussian noise, in opposition to a recent experiment [8]. Using the parameters extracted from the which-path measurements, we are able to calculate the dephasing resulting from thermal noise (instead of shot noise). The result is in perfect agreement with our recent measurements of the finite temperature coherence length [9]. Moreover, the magnetic field dependence of the coherence length is shown to result from a variation of the coupling between the two edges. Finally, we have developed a theory which gives a full scheme of the dephasing mediated by the electronic noise.

The interferences are obtained using an electronic Mach-Zehnder Interferometer (MZI) which was patterned on a high mobility two dimensional electron gas at a GaAs/Ga_{1-x}Al_xAs heterojunction (density $n_S = 2.0 \times 10^{11} \text{cm}^{-2}$ and mobility $\mu = 2.5 \times 10^6 \text{cm}^2/\text{Vs}$). Measurements have been done in the quantum Hall regime, at filling factor 2 (with a magnetic field $B=5.2 \text{ T}$). In the edge states, the electrons have a chiral motion with a drift velocity of the order of $10^4 - 10^5 \text{ ms}^{-1}$. A SEM view of the sample as well as a schematic representation of the two edge states are shown in Fig. 1a. The outer incoming edge state is split by G1 in two paths (a) and (b), which are recombined at G2 leading to interferences. SG is a side gate used to change the surface S defined by the two arms of the interferometer. The current which is not transmitted through the MZ, $I_R = I_0 - I_T$, is collected to the ground via the inner ohmic contact. The differen-

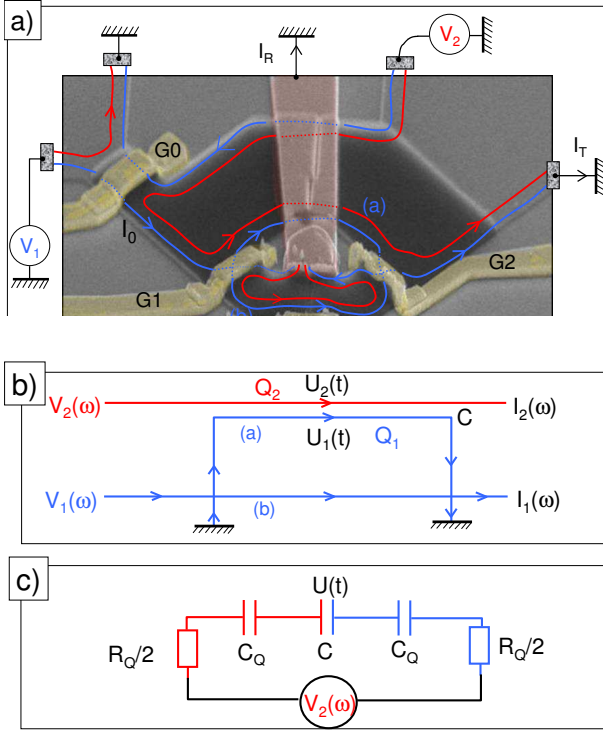


FIG. 1: (color online) **a)** Tilted SEM view of the device, with schematic representation of the edge states. G1 and G2 are Quantum Point Contact (QPC) which define the two beam splitters of the Mach-Zehnder interferometer. They are set to transmission $\mathcal{T}_1 \sim \mathcal{T}_2 \sim 1/2$ for the outer channel, while fully reflecting the inner channel. The two arms (a) and (b) are $L=11.3 \mu\text{m}$ long defining a surface S of $34 \mu\text{m}^2$. The small inner ohmic contact is connected to the ground via an Au metallic bridge. SG is a side gate. G0 is an additional beam splitter which makes it possible to bias the inner edge state by V_2 , while the other is biased by V_1 . G0 is tuned such that the outer channel is fully reflected, while the inner is transmitted with a probability \mathcal{T}_0 . **b)** Schematic representation of the edge states coupled by a geometrical capacitance C . **c)** Low frequency equivalent circuit with V_1 set to 0 V. $V_2(\omega)$ can be either generated by shot noise or by thermal noise, $C_Q = \tau/R_Q$ and $R_Q = h/e^2$ (see text).

tial transmission $\mathcal{T} = dI_t/dI_0$ have been measured at low temperature (~ 20 mK) by standard lock-in techniques with an AC voltage ($V_1 \sim 1 \mu\text{V}_{RMS}$ at 619 Hz).

It is straightforward to show that $\mathcal{T} \propto [1 + \mathcal{V} \sin(\varphi)]$, \mathcal{V} being the visibility and φ the Aharonov-Bohm (AB) flux through the surface S of the MZI [9]. In the present study we tuned the transmission \mathcal{T}_1 and \mathcal{T}_2 of the beam splitters G1 and G2 to $1/2$ in order to have a maximum visibility. The interferences are revealed by varying φ . It can be done either by applying a voltage V_{SG} on the side gate, or by applying a voltage V_2 on the inner edge state (playing here a role similar to the side gate). In Fig. 2, we have plotted the interference pattern obtained by the two methods. The periodicity V_0 of interferences with respect to V_2 depends on the coupling between the two

edge states which will be shown to be related to the time of flight τ through the MZI. In Fig. 4, one can notice that V_0 exhibits a large (up to a factor 3) non monotonous variation with the magnetic field on the Hall plateau at $\nu = 2$.

Any fluctuations on V_2 blur the phase. For a Gaussian distribution of the phase (we will discuss this notion later), the visibility is proportional to $e^{-\langle \delta\varphi^2 \rangle / 2}$ [10] where $\langle \delta\varphi^2 \rangle$ is the variance of the Gaussian distribution. It is simply related to the noise power spectrum S_{22} of V_2 through the coupling constant and the (unknown) bandwidth $\Delta\nu$: $\langle \delta\varphi^2 \rangle = (2\pi)^2 \langle \delta V_2^2 \rangle / V_0^2 = (2\pi)^2 S_{22} \Delta\nu / V_0^2$. If one generates partition noise on the inner edge state tanks to the splitter G_0 , the resulting excess noise $\Delta S_{22} = 2eR_Q \mathcal{T}_0 (1 - \mathcal{T}_0) V_2 [\coth(eV_2 / (2k_B T)) - 2k_B T / (eV)]$ [11, 12] leads to a visibility decreasing exponentially with V_2 when $eV_2 \gg k_B T$:

$$\mathcal{V} = \mathcal{V}_0 e^{-\mathcal{T}_0(1-\mathcal{T}_0)(V_2 - 2k_B T/e)/V_\varphi}, \quad (1)$$

with

$$V_\varphi^{-1} = \frac{4\pi^2 e R_Q}{V_0^2} \Delta\nu, \quad (2)$$

and $R_Q = 1/G_Q = h/e^2$.

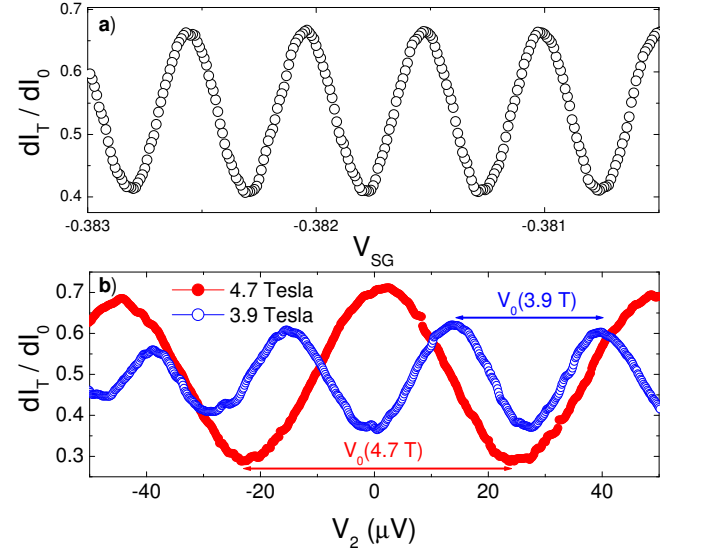


FIG. 2: (color online) **a)** Phase sweeping by varying the side gate voltage V_{SG} . **b)** Phase sweeping of the interferometer upon varying V_2 with $\mathcal{T}_0 = 1$ for two different magnetic fields. The periodicity V_0 of interferences depends on the magnetic field as shown in Fig. 4.

In Eq. 1, the unknown parameter is V_φ which is related to the bandwidth $\Delta\nu$ (Eq. 2). This approach for the dephasing is valid only if $\Delta\nu$ is such that the fluctuations lead to a Gaussian distribution of φ . It implies that many electrons have to be involved in the dephasing during the measuring time $1/\Delta\nu$, namely that

$\max(eV_2, 2k_B T) \gg h\Delta\nu$. This condition coincides with the fact that the noise power spectrum S_{22} can be considered as frequency independent. Note that the dephasing rate increases with V_2 because the number of involved electrons increases, not because the coupling between electrons increases with V_2 (as claimed in [8]). Fig. 3 shows that our data are in remarkable agreement with Eq. 2. In Fig. 3a we have plotted the visibility versus V_2 when $\mathcal{T}_0 = 1/2$, for two different magnetic fields. \mathcal{V} decreases exponentially with V_2 . The solid lines are fits to the data using an electronic temperature of 25 mK (for a fridge temperature of 20 mK). V_φ and \mathcal{V}_0 are the fitting parameters. The values of V_φ deduced from these measurements depend on the magnetic field in the same way as V_0 . In fact, V_φ is found to be proportional to V_0 (see Fig. 4). The slope of the exponential decrease is modified by the transmission of the beam splitter following a $\mathcal{T}_0(1 - \mathcal{T}_0)$ law. Fig. 3b shows the visibility for different values of V_2 and \mathcal{T}_0 at a magnetic field of 4.6 Tesla. The solid lines are fits to the data using Eq.1 with $V_\varphi = 7.2 \mu\text{V}$ and $T = 25 \text{ mK}$. Clearly, at high bias there is no V-shape contrary to what has been recently observed in ref.[8]. Instead, the curves show that the Gaussian approximation is valid. Note that the agreement with our theory is perfect when \mathcal{T}_0 is well defined in our sample. The dispersed data on the edges in Fig. 3b coincide to a strong dependence of \mathcal{T}_0 with the voltage applied on G0, resulting on an energy dependent transmission \mathcal{T}_0 [8].

We now compare the exponential decrease of the visibility in presence of shot noise with our recent observation that the coherence length of edge states is inversely proportional to the temperature [3]. When $eV_2 \ll k_B T$, the noise is dominated by the Johnson-Nyquist noise $S_{22} = 4k_B T R_Q$. One obtains:

$$\mathcal{V} = \mathcal{V}_0 e^{-T/T_\varphi} \text{ with } T_\varphi^{-1} = \frac{2 \times 8\pi^2 k_B R_Q}{V_0^2} \Delta\nu. \quad (3)$$

Here, the factor 2 arises from the fact that the two arms of the interferometer suffer from a coupling with a noisy inner channel, instead of one when creating partitioning. From equations 2 and 3, one gets:

$$eV_\varphi = 4k_B T_\varphi \quad (4)$$

Fig. 4, which is our main result, shows that Eq. 4 is in very good agreement with our data. This demonstrates for the first time that thermal noise and coupling between the two edge states are responsible for the finite coherence length measured recently [3].

This figure also brings a valuable point for the understanding of the underlying physics: the proportionality of V_φ to V_0 . This may be surprising at first sight: if $\Delta\nu$ were constant, according to Eqs. 2 and 3, V_φ would

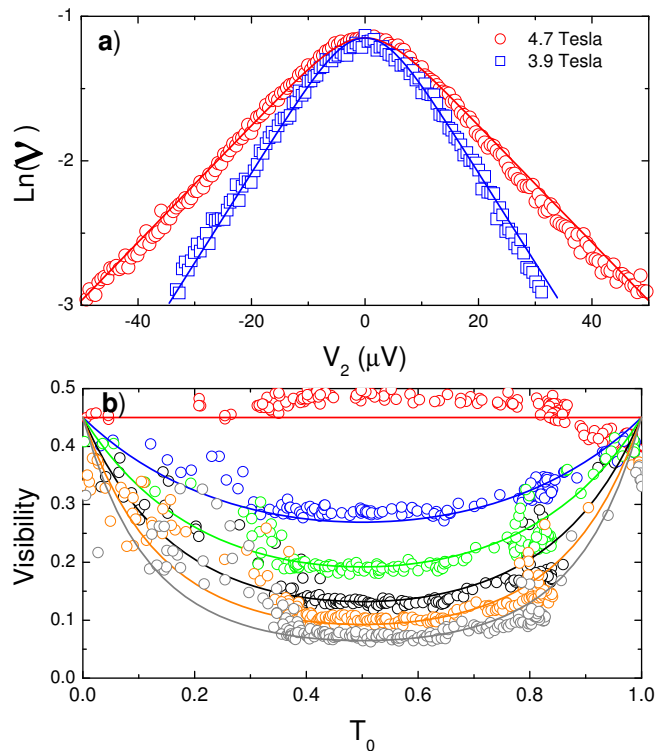


FIG. 3: (color online) **a)** Visibility decrease of the interferometer as a function of V_2 at $\mathcal{T}_0 = 1/2$ for two different magnetic fields 4.7 and 3.9 T. The solid lines are fits to the data $\mathcal{V} = \mathcal{V}_0 e^{-2\pi^2 \Delta S_{22} \Delta\nu / V_0^2}$ with an electronic temperature of 25 mK (for a base temperature of 20 mK) and $\mathcal{T}_0 = 1/2$. The high bias fit of the exponential decrease $\mathcal{V} = \mathcal{V}_0 \exp(-\mathcal{T}_0(1 - \mathcal{T}_0)V_2/V_\varphi)$ allows us to determine V_φ which is found to depends on the magnetic field. **b)** Visibility decrease of the interferometer as a function of \mathcal{T}_0 for $V_2=0, 21, 31, 42, 53$ and $63 \mu\text{V}$ from top to bottom. The solid lines are fits to the data using Eq. 1 with $\mathcal{V}_0=0.45$, $V_\varphi = 7.2 \mu\text{V}$ and $T = 25 \text{ mK}$.

scale as V_0^2 . Instead, as seen in Fig. 4, V_φ is proportional to V_0 . We will show that, varying the magnetic field changes the time of flight τ through the MZI, thus changing both the coupling between the edge states and the bandwidth $\Delta\nu$. This accounts for the proportionality of V_0 and V_φ . From the measurements of V_0 and V_φ , one can deduce using Eq. 2 that $h\Delta\nu$ varies from ~ 3 to $\sim 7 \mu\text{eV}$ when changing the magnetic field. This value of $h\Delta\nu$ is $\lesssim 2k_B T$, which validates our approach of Gaussian and white noise [14].

We now turn to a theoretical approach that relates V_0 and $\Delta\nu$ to microscopic parameters of the system and explains why $\Delta\nu \propto V_0$. We first consider the capacitive coupling between edge states. The influence of a gate coupled to one arm of the interferometer can be modelled in two equivalent ways. One can either consider that a gate voltage changes the surface S of the MZI without modifying the potential U_1 felt by the electrons, or that it adds an excess charge [4, 10, 13] which modifies U_1

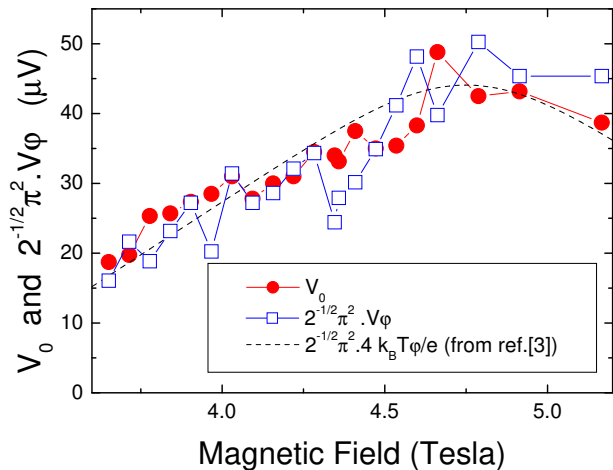


FIG. 4: (color online) V_0 and $\pi^2 V_\varphi / \sqrt{2}$ as a function of the magnetic field. The dashed line is the general behavior of $4k_B T_\varphi / e$ (right scale) measured in ref.[3], on the same sample.

without changing S . In this picture, the phase changes by $\varphi = \int_0^\tau eU_1 dt / \hbar$, where $\tau = L/v_D$ is the time of flight through the MZI and L stands for the length of one arm of the interferometer. This last relation allows to relate the phase noise $S_\varphi(\omega)$ to the potential noise $S_{U_1 U_1}(\omega)$:

$$S_\varphi(\omega) = 4 \frac{e^2}{\hbar^2} S_{U_1 U_1}(\omega) \frac{\sin^2(\omega\tau/2)}{\omega^2}. \quad (5)$$

We now determine the relation between the potential $U_1(t)$ and the electrochemical potential $V_2(t)$, following the lines of ref.[4]. In Fig. 1b, we have represented Q_1 as the charge on the arm (a) capacitively coupled through C to the inner channel with a charge Q_2 . The total charge on the capacitance is the sum of an emitted charge and a screening charge: $Q_j(\omega) = iG_Q(1 - e^{i\omega\tau})[V_j(\omega) - U_j(\omega)]/\omega$, with $G_Q = e^2/h$, $j = 1, 2$ and $x(t) = \int x(\omega)e^{-i\omega t} d\omega$. From the charge neutrality $Q_1 = -Q_2$ and the $U(\omega) = U_2(\omega) - U_1(\omega) = Q_2(\omega)/C$, one gets

$$G_{12} = \frac{dI_1(\omega)}{dV_2(\omega)} = \frac{G_Q(1 - e^{i\omega\tau})}{2 + iG_Q(1 - e^{i\omega\tau})/(\omega C)}. \quad (6)$$

This result is similar to the one obtained in [4], with differences in the charge relaxation resistance: it arises both from the chirality of the edge state ($R_Q/2$ instead of two $R_Q/2$'s in parallel) and from the non "perfect" gate that forms the inner edge state (two $R_Q/2$'s in series). The low frequency equivalent circuit (Fig. 1c) leads to $U_1 = V_2/(C_Q/C + 2)$ for dc biasing, $C_Q = G_Q\tau$. Then the periodicity V_0 is related to τ by :

$$V_0 = (2 + 1/\gamma) \frac{h}{e\tau}, \quad (7)$$

with $\gamma = C/C_Q$. As $C \propto L$ and $C_Q \propto L/v_D$, γ should varies like v_D . Finally, the finite frequency transconductance $G_{12}(\omega)$ allows to relate the potential fluctuations

to the electrochemical fluctuations:

$$S_{U_1 U_1}(\omega) = \frac{1}{4} |1 - G_{12}(\omega)i/\omega C|^2 S_{22}(\omega). \quad (8)$$

We now consider the case of white partition noise $S_{22} = 2eR_Q V_2 \mathcal{T}_0(1 - \mathcal{T}_0)$ or white thermal noise $S_{22} = 2 \times 4k_B R_Q T$. Finally, using Eqs. 5 and 8 with $\tau/\tau_\varphi = < \delta\varphi^2 > / 2$, one finds:

$$\frac{1}{T_\varphi} = \frac{8k_B}{\hbar} \tau \mathcal{I}(\gamma) \quad \text{and} \quad \frac{1}{V_\varphi} = \frac{2e}{\hbar} \tau \mathcal{I}(\gamma) \quad (9)$$

with,

$$\mathcal{I}(\gamma) = \int_0^\infty \frac{\sin^2(x)\gamma^2}{\sin^2(x) + 2\gamma x \sin(2x) + 4\gamma^2 x^2} dx.$$

We see here that both the dephasing rate described by V_φ and T_φ and the phase sensitivity to the potential of the inner edge state described by V_0 are proportional to the time of flight τ . For $\gamma \ll 1$, $\mathcal{I}(\gamma) \sim \gamma\pi\sqrt{2}/8$. Then, using Eqs. 7 and 9,

$$V_\varphi^{-1} = \frac{\pi^2}{\sqrt{2}} \times V_0^{-1}. \quad (10)$$

One can see, in Fig. 4, that our theory is in excellent agreement with our measurements. Moreover, at first order, the ratio between V_0 and V_φ is independent of the coupling parameter γ . It is not possible to conclude on the exact origin of magnetic field variations of the coupling. It may arise from the disorder which modifies the effective trajectory length and hence the time of flight. The agreement between experiment and theory is very good as far as $\gamma \lesssim 0.2$, which corresponds to reasonable values of the capacitance and the drift velocity [9]. One can notice that $\tau_\varphi^{-1} \propto \gamma$ when $\gamma \ll 1$. Then, increasing the coupling (or reducing the screening) increases γ and thus $1/\tau_\varphi$: the poor screening in the IQHE is actually responsible for the limited coherence time in the edge states.

To conclude, we have shown that the coherence length of the edge states at filling factor 2 is limited by the Johnson-Nyquist noise. Changing the magnetic field makes it possible to modify the coupling between the edge states and thus modifies the coherence length. Our results are well described by a mean-field approach that relates the phase randomization to the fluctuations of the electrostatic potential in the interferometer arms.

The authors would like to thank Markus Buttiker for fruitful discussions.

-
- [1] Y. Ji *et al.*, Nature **422**, 415 (2003).
 - [2] I. Neder *et al.*, Nature **448**, 333 (2007).
 - [3] P. Roulleau *et al.*, arXiv:0710.2806v2 (to be published in Phys. Rev. Lett.).

- [4] G. Seelig and M. Buttiker, Phys. Rev. B **64**, 245313 (2001).
- [5] S. E. Barrett, Phys. Rev. Lett. **74**, 5112 (1995).
- [6] T. Martin and S. Feng, Phys. Rev. Lett. **64**, 1971 (1990).
- [7] D. C. Dixon *et al.*, Phys. Rev. B **56**, 4743 (1997).
- [8] I. Neder *et al.*, Nature Physics **3**, 534 (2007).
- [9] P. Roulleau *et al.*, Phys. Rev. B **76**, 161309 (2007).
- [10] A. Stern, Y. Aharonov, and Y. Imry, Phys. Rev. A **41**, 3436 (1990).
- [11] T. Martin and R. Landauer, Phys. Rev. B **45**, 1742 (1992).
- [12] M. Büttiker, Phys. Rev. B **46**, 12485 (1992).
- [13] D. Rohrlich *et al.*, Phys. Rev. Lett. **98**, 096803 (2007).
- [14] It can lead to a small deviation from our theory at the lowest temperature (20 mK) when $eV_2 \leq 2k_B T$.